scientific reports

Check for updates

OPEN

Green synthesis of silver nanoparticles from pomegranate peel and their application in PVA-based nanofibers for coating minced meat

Burcu Sari Gencag[1,2]✉, Kevser Kahraman[3] & Lutfiye Ekici[4]

In this study, silver nanoparticles (AgNPs) were synthesized via a green method from pomegranate peel extract and incorporated into polyvinyl alcohol (PVA) to produce AgPVA nanofibers through electrospinning. Nanofibers containing different silver concentrations (0.5, 1, and 1.5% Ag) were used as coating materials to coat minced meat, and their effects on various quality parameters during storage at 4 °C were evaluated. FTIR, XRD, SEM, and antibacterial analyses were conducted for the characterization of AgNPs and AgPVA nanofibers. To assess the quality characteristics of the minced meat during storage, pH, color, peroxide, TBARS, and microbiological analyses were performed. The results indicated that silver concentrations up to 1% could delay oxidation in minced meat and help preserve its quality. Compared with the other samples, the samples coated with 0.5% AgPVA (A1) and 1.0% AgPVA (A2) nanofibers exhibited a significant antimicrobial effect at the 6-day storage point ($p < 0.05$). The migration of AgNPs into minced meat was monitored during storage, and all migration values remained below the European food safety authority (EFSA) safety limit of 0.05 mg/kg, demonstrating the safety of the coatings. These findings suggest that AgPVA nanofibers synthesized via a green method could be a promising approach for extending the shelf life of perishable foods by reducing spoilage.

One of the most effective methods for ensuring food safety and preventing foodborne illnesses is the utilisation of food packaging. In recent years, there has been a notable shift in consumer and producer awareness, with increasing demand for minimally processed foodstuffs and a growing emphasis on sustainability. This has led to significant interest in the development of biodegradable materials, particularly in sectors such as healthcare, agriculture, and food processing[1]. Increased awareness of green packaging and government regulations has led to the research and development of biodegradable natural materials[2].

The use of nanotechnology in food packaging systems has been extensively researched and developed with the aim of monitoring product conditions at every stage of the food production and consumption process[3]. Nanotechnology has revolutionized food packaging systems, allowing for the development of nanocomposite materials with enhanced properties. Active packaging systems, in particular, interact with food and its environment to maintain sensory and microbiological quality while extending shelf life[4].

There is a strong demand for the development of safe, biodegradable, and environmentally friendly active food packaging materials. Among these alternatives, the electrospinning technique stands out as a promising candidate[5]. This technology uses electrostatic force to generate an electrically charged jet of viscoelastic polymer solution, which forms an ultrathin structure upon solvent evaporation[6]. The process of integrating different food packaging materials with nanoparticles has recently gained popularity in the food packaging industry. These nanocomposites not only exhibit outstanding antibacterial properties but also demonstrate good mechanical performance and strong resistance characteristics[7]. Nanoparticles (NPs) have gained significant attention in food packaging due to their potential to improve the mechanical, thermal, and antimicrobial properties

[1]Department of Food Engineering, Graduate School of Natural and Applied Sciences, Erciyes University, 38039 Kayseri, Turkey. [2]Department of Gastronomy and Culinary Arts, Cappadocia University, 50240 Nevşehir, Turkey. [3]Department of Materials Science and Nanotechnology Engineering, Engineering Faculty, Abdullah Gül University, 38080 Kayseri, Turkey. [4]Department of Food Engineering, Engineering Faculty, Erciyes University, 38039 Kayseri, Turkey. ✉email: burcu.sari@kapadokya.edu.tr

of packaging materials. Recent studies have demonstrated the application of nanoparticles such as silver[8], titanium dioxide[9], and zinc oxide[10] in active food packaging systems, where they play a key role in extending shelf life by inhibiting microbial growth and preventing spoilage[11]. Among these, silver nanoparticles (AgNPs) are particularly valued for their strong antimicrobial effects against a broad spectrum of pathogens, making them a popular choice in food packaging applications[12]. In recent years, interest in synthesizing AgNPs via plant extracts as an environmentally friendly, cost-effective, and reliable alternative to chemical methods has increased[13]. Nanofibers containing nanoparticles have emerged as a novel solution in food packaging, offering ultrathin structures with enhanced barrier and antimicrobial properties. AgNP-based antimicrobial packaging is a form of active food packaging that plays a significant role in extending the shelf life of various food products[12]. Numerous researchers have investigated the effects of silver nanoparticles on various food items, including meat, poultry, dairy, and fruits[14–19].

AgNPs synthesized through biological methods are often highlighted as a safer, cost-effective, and environmentally sustainable alternative to conventionally produced nanoparticles. These biologically synthesized nanoparticles are typically derived using green materials, including plant extracts, enzymes, and microorganisms, which align with the principles of green chemistry[20]. Despite their potential, the primary concern regarding the use of nanoparticles in food packaging remains their migration into food products, posing a risk similar to that of other heavy metals[21]. To ensure consumer safety, it is crucial to better understand the interaction between nanomaterials and food, as well as to comprehensively assess their migration behavior from packaging to food items[22].

To ensure food safety and protect environmental sustainability, various natural biodegradable polymers, such as chitosan and cellulose derivatives, have been utilised in food packaging. However, their limitations, including low water resistance and sensitivity to pH fluctuations, have driven increased interest in the application of synthetic biodegradable polymers[23]. Poly (vinyl alcohol) (PVA) is a hydrophilic polymer that has excellent chemical and thermal stability. PVA is a nontoxic, biocompatible, highly water-soluble, and biodegradable polymer that can easily be transformed into fibers through electrospinning. These unique properties make PVA an ideal candidate for applications in sustainable food packaging systems[24–27].

The pomegranate (*Punica granatum* L.) belongs to the *Punicaceae* family and is grown in warm regions worldwide[28]. Pomegranate peel is a rich source of antimicrobial agents, tannins, anthocyanin pigments, antioxidants such as catechins and polyphenols, ellagitannins, ellagic acid, gallic acid, and flavonoids[29]. These bioactive compounds have been reported to play a key role in the effective stabilization and reduction of metal ions into AgNPs[29–31].

The selection of pomegranate, watermelon, orange, and apple peels was based on their high content of bioactive compounds, which are essential for the green synthesis of silver AgNPs[32–34]. Additionally, Türkiye is a leading producer of these fruits, particularly pomegranate, orange, apple, and watermelon, which are grown abundantly across the country. As a result, the peels of these fruits are widely available as agricultural waste. Utilizing these wastes aligns with the principles of green chemistry and contributes to environmental sustainability.

The aim of this study was to identify the most suitable food waste for the synthesis of silver from pomegranate (*Punica granatum* L), watermelon (*Citrullus lanatus*), orange (*Citrus sinensis*), and apple (*Malus domestica*) peels. AgNPs were synthesized from the selected pomegranate peel, and AgPVA nanofibers were produced via the electrospinning method. The synthesized AgNPs and fibers were characterized, and the nanofibers were applied to minced meat to evaluate the effects of PVA-based coating on product quality.

Materials and methods

Preparation of extracts

Fresh pomegranate (*Punica granatum* L.), watermelon (*Citrullus lanatus*), orange (*Citrus sinensis*), and apple (*Malus domestica*) fruits were obtained from a local greengrocery in Nevşehir, Turkey. The fruits were thoroughly washed, and their peels were separated, and dried at 50 °C to reach a moisture content of 25–30%. Each peel was then ground into a powder via a food processor. Ten grams of each sample was weighed and heated with 100 mL of distilled water at 60 °C for 20 min. The samples were allowed to cool to room temperature and were then filtered first through coarse filter paper and subsequently through Whatman No. 1 filter paper. The resulting extracts were stored at 4 °C in a dark environment for future analysis[35].

Green synthesis of silver nanoparticles

Green synthesis of silver nanoparticles was conducted by mixing 10 mL of the extract with 90 mL of a 1 millimolar (mM) $AgNO_2$ solution, and the mixture was kept in the dark for 24 h at room temperature, as adapted from[35]. After the reaction was complete, the extract mixture was centrifuged at 14,000 rpm for 20 min. The solid residue obtained after centrifugation was washed with distilled water to remove excess silver, as commonly reported in green synthesis protocols using plant extracts[36,37]. This washing process is essential to remove unreacted silver ions (Ag^+) and by-products that could interfere with subsequent analyses and stability of the synthesized nanoparticles. The material was then dried in an oven at 50 °C for 24 h. The dried material was ground with a glass rod and stored at 4 °C in the dark for further characterization and antimicrobial activity testing.

Characterization of synthesized silver nanoparticles

The reduction of silver ions in the synthesized AgNPs was analyzed via a UV-vis spectrophotometer (Shimadzu UV 1800, Japan). The samples were measured at specific time intervals (1 h, 12 h, and 24 h) within the wavelength range of 300–700 nm. To identify the functional groups present in the green nanoparticles synthesized from pomegranate peels, FT-IR absorption spectra were recorded in the wavenumber range of 4000 –400 $^{-1}$using a SpotLight 400 FT-IR spectrometer (PerkinElmer, USA). The crystallinity and phase composition of the

synthesized AgNPs were examined via an X-ray diffractometer (Malvern Panalytical Ltd., UK) operating at 45 kV and 200 mA with Cu Kα radiation in the 2θ angle range of 5–90.

Antibacterial activity of synthesized silver nanoparticles

The antibacterial activity of AgNPs was investigated against a range of bacterial strains, including *Staphylococcus aureus* (ATCC 25923), *Bacillus cereus* (ATCC 11778), *Escherichia coli* (ATCC 25922), and *Pseudomonas aeruginosa* (Clinic isolate), using the agar well diffusion method. The bacteria were spread on Müller-Hinton agar media at a turbidity of 0.5 McFarland. Agar wells with a diameter of 6 mm were prepared and loaded with 50 µL of AgNPs solution at concentrations of 150, 75, 37.5, and 18.75 µg/mL. A well containing deionized water served as the negative control, while ampicillin was used as the positive control. The plates were incubated at 37 °C for 24 h, after which the diameter of the inhibition zone, indicated by a clear zone with no bacterial growth, was measured.

Preparation of AgPVA nanofibers by electrospinning

AgPVA nanofibers were produced via the electrospinning method, with 0.5%, 1%, and 1.5% (w/v) Ag nanoparticles added to polyvinyl alcohol (PVA), hydrolyzed at 87–89% (Sigma-Aldrich, USA) and prepared at a concentration of 10% (w/v) using distilled water as the solvent. The solutions prepared for production were transferred into a 5 mL plastic syringe and placed in a syringe pump. After multiple preliminary trials, the distance between the collector and the feed tip was set to 12 cm, the applied voltage was 12 kV, and the feed rate was 0.30 mL/hr, resulting in the production of AgPVA nanofibers.

Characterization of nanofibers

The morphologies of the films produced by electrospinning were examined by scanning electron microscopy (SEM) (Zeiss Evo LS-10, Germany). Before SEM analysis, the samples were coated with a thin layer of gold under vacuum conditions to increase the electrical conductivity of the nanofibers and obtain clearer images. The diameters of the nanofibers were measured at 100 randomly selected points and analyzed using ImageJ software. Additionally, energy-dispersive X-ray spectroscopy (EDXS) measurements were conducted to determine the types and quantities of elements present in the sample. The FT-IR absorption spectra of the AgPVA nanofiber were analyzed in the wavenumber range of 4000 –400 cm^{-1} using a SpotLight 400 FT-IR spectrometer (PerkinElmer, USA). The crystallinity and phase composition of the synthesized nanofibers were investigated using an X-ray diffractometer (Malvern Panalytical Ltd., UK) operating at 45 kV and 200 mA with Cu Kα radiation in the 2θ angle range of 5–90.

Antimicrobial activity of the nanofibers

A zone of inhibition test was conducted to determine the antimicrobial efficacy of the AgPVA nanofibers. The gram-positive bacteria *Bacillus cereus* and *Staphylococcus aureus*, as well as the gram-negative bacteria *Escherichia coli* and *Pseudomonas aeruginosa*, were selected. A 100 µL suspension of each bacterial strain was prepared at 0.5 McFarland turbidity and homogeneously inoculated onto Mueller-Hinton agar plates. The AgPVA nanofibers were placed on the surface of the agar plate. A 10% PVA nanofiber was used as the negative control, and an ampicillin disc served as the positive control. The Petri dishes were incubated at 37 °C for 24 h. After this period, the diameter of the inhibition zone around the samples was measured via a caliper.

Coating of minced meat samples with nanofiber film

Fresh minced meat samples derived from the chuck (shoulder) region of beef were obtained from a local supermarket (Migros) in Ürgüp, Türkiye. The meat was minced at the time of purchase to ensure uniformity. For the experiment, 20 g of minced meat was weighed for each sample, ensuring consistency across all groups. The samples were coated with nanofibers deposited on aluminum foil, ensuring complete coverage without removing the foil. The minced meat samples were divided into five groups and coated with nanofibers. These groups were defined as follows: P10: PVA nanofibers prepared at a 10% (w/v) concentration without silver; A1: AgPVA nanofibers with 0.5% (w/v) Ag; A2: AgPVA nanofibers with 1.0% (w/v) Ag; A3: AgPVA nanofibers with 1.5% (w/v) Ag; and NC: aluminum foil without nanofiber film. The samples were stored in a refrigerator at + 4 °C for 9 days, and quality analyses were performed on days 0, 3, 6, and 9.

Analyses performed on minced meat samples

The pH of all the minced meat samples was measured at three different points via a portable pH meter (Milwaukee, MW102-F, Romania) with an immersion-type probe. The cross-sectional color (L brightness, a redness, b* yellowness) was determined using a portable color meter (PCE-CSM 7, Germany) with four repetitions. The determination of peroxide in the test samples was carried out according to the method described by[38]. A quantity of 5 g of the sample was weighed and crushed with 30 mL of chloroform in a blender for 2 min. The mixture was filtered through Whatman No. 1 filter paper, and 30 mL of glacial acetic acid and 2 mL of saturated potassium iodide solution were added. The flask was then stirred for 2 min and kept in the dark for 5 min. After this waiting period, 100 mL of distilled water and 2 mL of 1% starch solution were added, and the solution was titrated with 0.1 N sodium thiosulfate. The peroxide values of the samples were expressed as milliequivalents of oxygen per kilogram (meq O_2/kg) of sample. The secondary products of lipid oxidation in the samples during storage were determined via the spectrophotometric TBA method described by[39]. Accordingly, 20 g of the sample was weighed into a beaker, 100 mL of 20% TCA solution was added, and the mixture was homogenized for 2 min. Then, 50 mL of cold water was added, and the mixture was further homogenized for 1 min. The mixture was filtered into a 100 mL flask using filter paper, and the flask was filled to a volume of 100 mL with a 1:1 TCA solution. A 5 mL aliquot was taken from the flask, and transferred to a test tube, and 5 mL of 0.02 M TBA

solution was added. The test tubes were incubated in a water bath at 80 °C for 35 min. For the blank sample, 5 mL of 1:1 TCA solution was added, and 0.02 M TBA was added. After the heating period, the absorbance values of the cooled samples were measured at 532 nm using a UV-vis spectrophotometer. The absorbance values were multiplied by a factor of 5.2 to calculate the TBA value in mg malondialdehyde/kg.

Assessment of the Microbiological characteristics of the minced meat samples

Total mesophilic aerobic bacteria count

The total mesophilic aerobic bacteria count (TMABc) was defined in accordance with the specifications set forth in the FDA's Bacteriological Analytical Manual (FDA-BAM). The number of TMABc was analyzed using the plate colony counting method. For this purpose, samples were removed from their coating after each storage period. Then, 10 g of samples from each group were homogenized for 150 s using a stomacher. After serial dilutions (10^1 to 10^8) were prepared, the samples were spread onto plate count agar (PCA, Merck-VM888763 930) and incubated at 35 °C for 48 h. The TMAB counts were expressed as log CFU/g[40].

Total psychrophilic bacteria count

The total psychrophilic bacterial count (TPBc) was determined following the FDA-BAM method. The same steps described in Sect. 2.10.1 were followed. The plates were incubated at 7 °C for 10 days, and the results are expressed as log CFU/g[40].

Migration of silver test

0.1–0.2 g sample is taken and 2 ml HNO_3 and 3ml H_2O_2 are added. A temperature and pressure program is applied in the microwave solubilizer (closed system). The clear solutions obtained are taken and diluted to 10 ml with pure water (MİLESTONE brand).

Before the analysis, standards are prepared at known concentrations (0, 1, 5, 10, 20, 30, 40, 50 ppb) containing the elements to be analyzed. To check the measurement parameters of the device, performance adjustment is made by passing tune solution (200 ppb Li, Yb, Cs) through the device. After the performance of the device is checked with the tune solution, the method containing the elements to be analyzed is selected and the standards are first introduced to the device, then the analysis of the solubilized and diluted samples is started. Analysis representing the entire periodic table during analysis. Apart from the elements to be determined, the solution containing 200 ppb internal standard elements (Sc, In) is fed to the device. Dissolved samples are analyzed on an Agilent 7900 ICP MS instrument.

Statistical analysis

The statistical analysis of the data was performed using the SPSS software for windows (SPSS 25.0 for Windows; SPSS Inc. Chicago, IL, USA) package at a 95% confidence interval. The data from each experiment were analyzed using ANOVA and Duncan's Post-Hoc tests.

Results and discussion

Characterization of AgNPs

The synthesis of AgNPs from pomegranate peel was first indicated by a color shift in the solution, which changed from pale yellow to a yellowish-brown hue[35,41]. The spectra of watermelon, pomegranate, apple, and orange samples after synthesis, revealed that the pomegranate sample presented the highest peak between 400 and 450 nm across all three time intervals. The presence of a distinct peak within this range, characteristic of AgNPs, along with the observation of the optimal brown color, confirms the presence of AgNPs[42–44]. Moreover, the stability of the pomegranate sample at a wavelength of approximately 450 nm after 24 h further indicates that stable nanoparticles were produced.

The FTIR spectrum of the biosynthesized AgNPs shows multiple absorption peaks corresponding to various functional groups, such as hydroxyl, carbonyl, and amine groups, which are responsible for the reduction and stabilization of AgNPs[45,46]. These functional groups are essential for the reduction and stabilization of AgNPs, contributing to their high stability and reactivity for diverse applications such as photocatalytic dye degradation and antimicrobial activity[46–48]. Figure 1 shows the FT-IR measurements used to determine the reduction of Ag ions to AgNPs.

Strong vibrational bands of AgNPs were observed at 2971, 2307, 1879, 1576, 1247, 993, and 517 cm^{-1}. The peak at 2917.2 cm^{-1} typically corresponds to C–H stretching vibrations, which are commonly found in the aliphatic chains of organic compounds[41,49]. The value at 2307.7 cm^{-1} typically indicates the occurrence of C≡N stretching vibrations[50]. The peak at 1879.0 cm^{-1} is associated with carbonyl groups (C=O stretching), although peaks at this wavelength are less common. These peaks may indicate specific structures, such as metal-carbonyl complexes[51]. The peak at 1576.3 cm^{-1} corresponds to the C=C stretching vibration band in aromatic compounds, indicating the presence of aromatic rings[52]. The peak at 1247.4 cm^{-1} typically indicates C–O–C stretching vibrations, which may suggest the presence of structures such as esters or ethers[53,54]. The peak at 993.15 cm^{-1} typically indicates C–H bending vibrations, suggesting the presence of aromatic rings or alkenes[55]. A peak at 517.13 cm^{-1} indicates the presence of metal-oxygen (M-O) or metal-sulfur (M-S) bonds. Indeed, owing to the substantial mass of silver, infrared radiation emitted at low energies is capable of vibrating the oxide or nitride bonds of this element. Given the direct relationship between the energy of electromagnetic radiation and its wavenumber, it can be concluded that bonds involving the silver element vibrate at low wave numbers. A comparison of the spectra indicates that the enhanced peak intensity at wavenumbers below 700 cm^{-1} is likely attributable to the presence of silver-containing bonds[41]. This finding provides evidence supporting the successful synthesis of AgNPs.

X-ray diffraction (XRD) analysis, shown in (Fig. 2), revealed that the synthesized AgNPs possessed a face-centered cubic (FCC) crystal structure. The positions at 38, 44, 65, and 77° corresponded to the (111), (200),

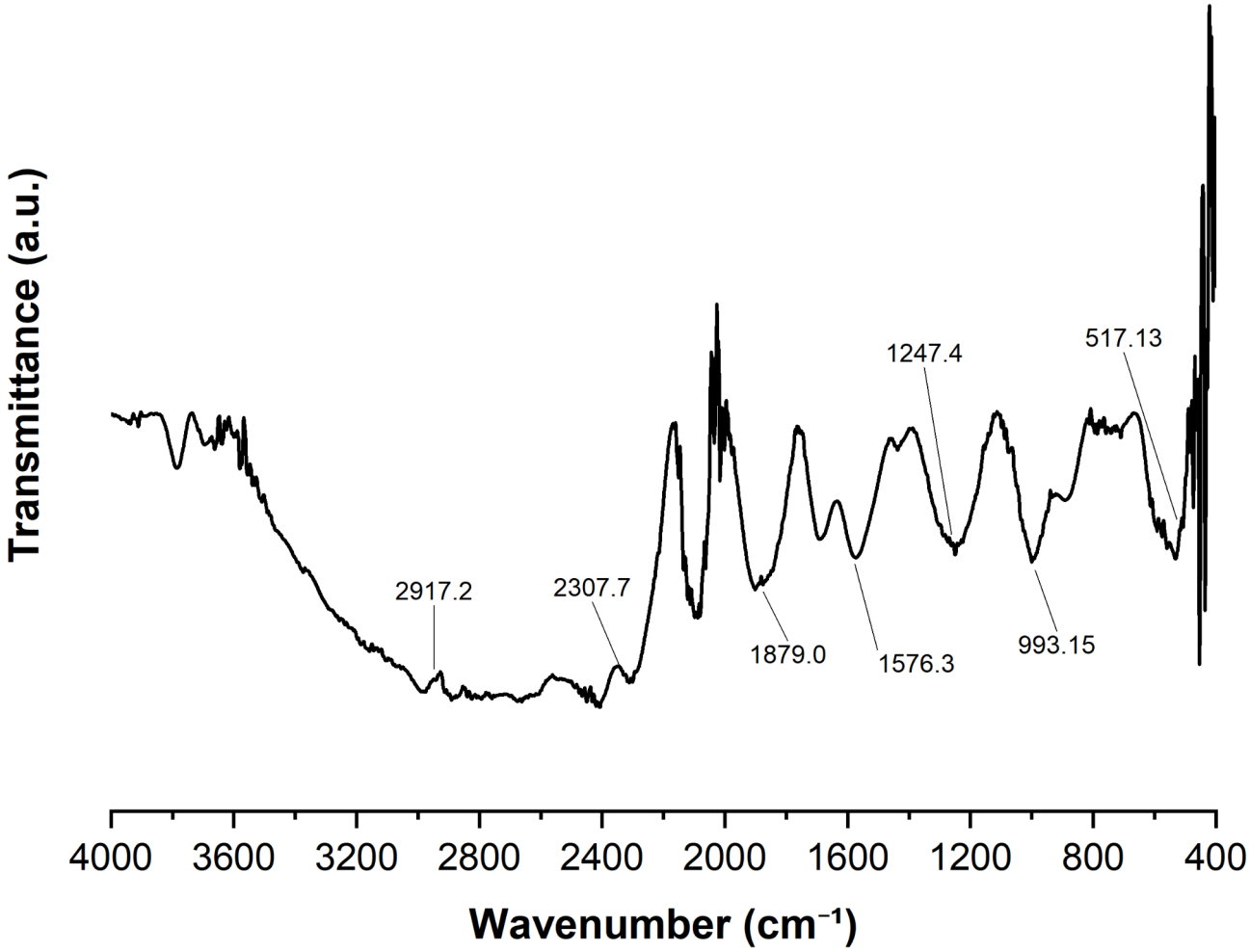

Fig. 1. FT-IR spectra of AgNPs synthesized from pomegranate peel extract.

(220), and (311) planes, respectively. It has been documented in the literature that these peaks correspond to the crystal surfaces of the face-centered cubic (FCC) form of silver[56]. The XRD noise can be attributed to the presence of complex biomolecules originating from the fruit peel extract[35]. The AgNP sample exhibits the (111) plane, which is the typical high-density peak for a face-centered cubic (FCC) structure. The high degree of crystallinity of the AgNP is reflected in the peak intensity[57]. A comparison of the XRD results with those of previous studies in the literature revealed that the obtained XRD results were consistent with the literature[57–60].

Antibacterial activity of synthesized AgNPs

AgNPs have long been acknowledged as broad-spectrum antimicrobial agents. Research has demonstrated that AgNPs exhibit strong antibacterial activity against both Gram-positive and Gram-negative pathogenic bacteria[61]. Furthermore, studies have reported that the antibacterial efficacy of nanoparticles and their effective concentrations are largely influenced by the synthesis method, particle size, and specific bacterial strains being investigated[62,63].

In this study, the antibacterial activity of AgNPs was evaluated against various bacterial strains, including *Staphylococcus aureus* (ATCC 25923), *Bacillus cereus* (ATCC 11778), *Escherichia coli* (ATCC 25922), and *Pseudomonas aeruginosa* (clinic isolate). The results revealed that the antibacterial activity against all test bacteria was sensitive to increasing AgNP concentrations (Table 1; $p < 0.05$). Thus, as the concentration of nanoparticles increased, the inhibition of bacterial growth gradually increased (Table 1; Fig. 3). The greatest antibacterial effect of the AgNPs was observed against *Staphylococcus aureus* and *Pseudomonas aeruginosa*. A comparison of the inhibition zones of *Staphylococcus aureus* and *Escherichia coli* with those of ampicillin revealed that although the activity of AgNPs was lower than that of ampicillim, they still exhibited notable inhibition. A comparison of the inhibition zones of *Bacillus cereus* and *Pseudomonas aeruginosa* with those of ampicillin revealed that AgNPs were more effective.

The development of an inhibition zone is dependent on the diffusion rate of the antibacterial agent and the growth rate of the microorganism. The appearance of halos with diameters of 10 mm or more signifies the presence of inhibitory activity[35]. The inhibition diameter ranged from 10.18 to 12.84 mm in the highest

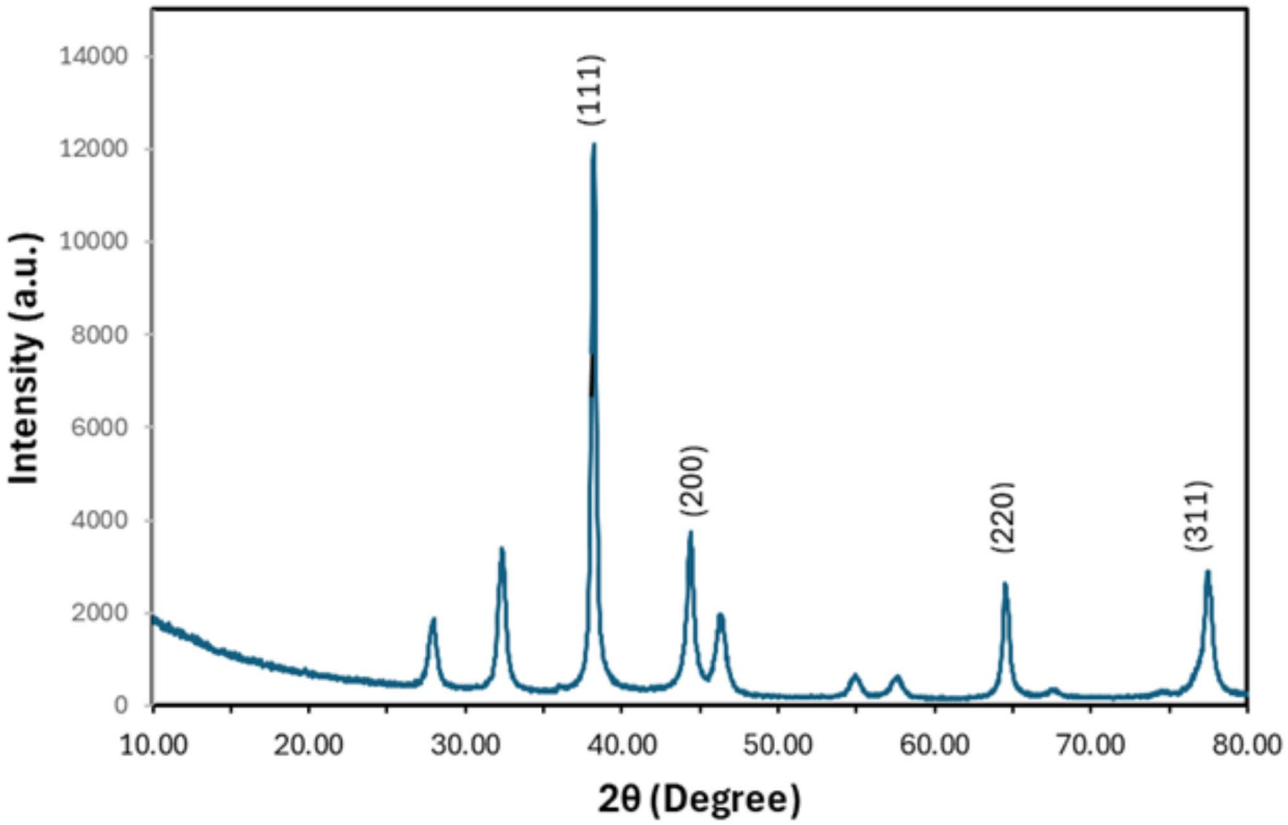

Fig. 2. XRD pattern of the AgNPs obtained from pomegranate peel extract.

Bacteria	Diameter of inhibition zone (mm) ± SD			Ampicilin
	150 µg/ml	75 µg/ml	37.5 µg/ml	18.75 µg/ml
Staphylococcus aureus	12.52 ± 0.24[a]	11.95 ± 0.10[a]	10.97 ± 0.03[b]	10.44 ± 0.39[a]
Bacillus cereus	10.84 ± 0.14[b]	10.26 ± 0.19[b]	10.25 ± 0.23[c]	9.15 ± 0.16[b]
Escherichia coli	10.18 ± 0.06[c]	9.87 ± 0.36[b]	9.40 ± 0.15[d]	9.21 ± 0.09[b]
Pseudomonas aeruginosa	12.84 ± 0.48[a]	11.92 ± 0.39[a]	11.74 ± 0.31[a]	10.62 ± 0.62[a]

Table 1. Well agar diffusion test of AgNPs from *Staphylococcus aureus*, *Bacillus cereus*, *Escherichia coli* and *Pseudomonas aeruginosa*. [a–d]Different letters in the same column indicate a significant difference ($P < 0.05$). The data are presented as the means ± standard errors.

concentration solution (150 µg/mL) and from 9.15 to 10.62 mm in the lowest concentration solution (18.75 µg/mL).

Many studies have explored the antibacterial mechanisms of AgNPs, with one of the primary mechanisms being the release of silver ions (Ag^+). These ions bind to the bacterial cytoplasm and cell wall via electrostatic interactions and have an affinity for sulfur-containing proteins, significantly enhancing membrane permeability. The uptake of free Ag^+ by bacterial cells triggers the generation of reactive oxygen species (ROS), which exacerbates membrane damage and induces DNA alterations. In addition, Ag^+ ions can inhibit protein synthesis and affect signal transduction pathways. Smaller nanoparticles are able to penetrate the bacterial cell wall, resulting in cell lysis. However, the formation of bacterial capsules and biofilms often impedes the transfer of Ag^+ ions or AgNPs, providing bacteria with protection against these agents[61,63,64].

Characterization of the AgPVA nanofibers

The functional groups of the produced nanofibers were characterized using FTIR spectroscopic analysis, and the resulting spectra are presented in (Fig. 4).

The prominent O–H stretching vibrations were observed in the 3400–3900 cm^{-1} range, specifically at 3279.1, 3288.3, 3305.5, and 3312.0 cm^{-1} across all samples, indicating that the hydroxyl groups of PVA remained intact despite the incorporation of Ag nanoparticles. Minor shifts in these peaks were noted as the silver concentration increased, which may be attributed to interactions between the hydroxyl groups of PVA and the Ag nanoparticles.

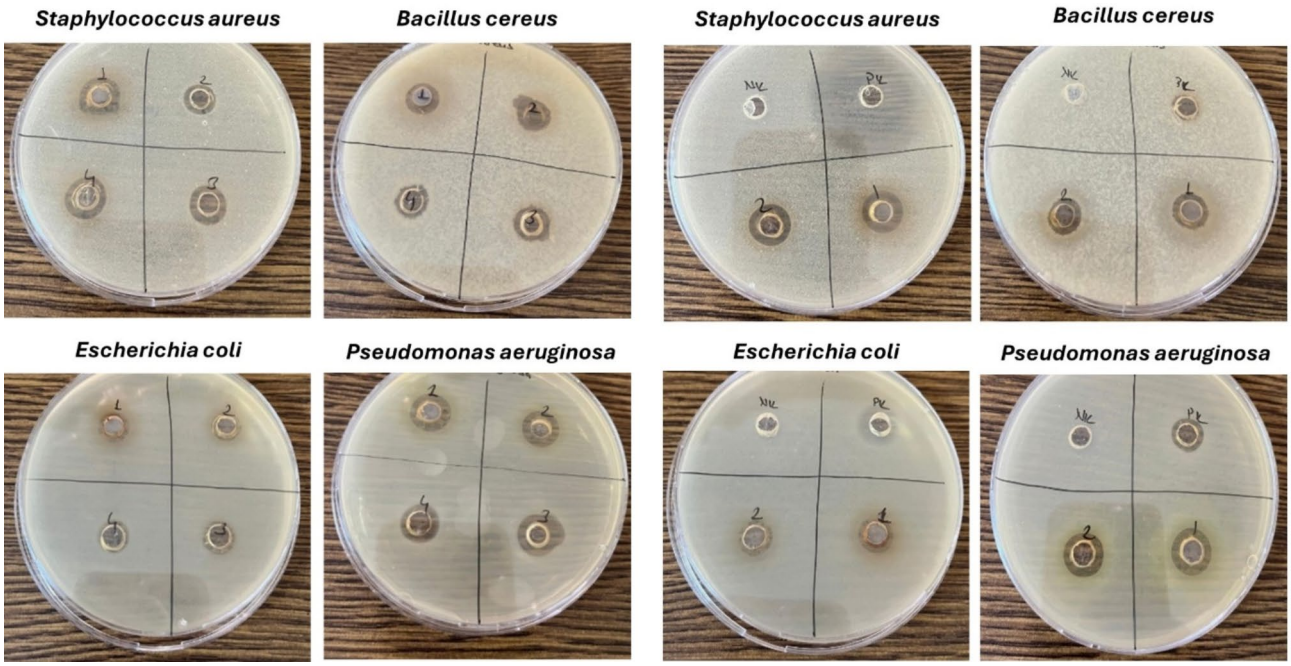

Fig. 3. The antibacterial activities of AgNPs were evaluated at concentrations of 150, 75, 37.5, and 18.75 µg/mL(1,2,3 and 4, respectively). The central wells of each plate were filled with deionized water as the negative control and ampicillin (150 µg/mL) as the positive control.

The C–H stretching vibrations (around 2915.1–2951.6 cm^{-1}) also showed slight shifts, likely due to changes in the polymer matrix structure caused by AgNP incorporation. Additionally, the C=O stretching vibrations, indicative of ester or carbonyl groups, appeared in the 1730–1714 cm^{-1} region and shifted significantly with increasing Ag content, suggesting chemical changes in the matrix.

The peaks observed in the lower wavelength regions (500–600 cm^{-1}) confirmed the presence of Ag–O vibrations, further supporting the integration of AgNPs into the PVA matrix. These results collectively align with previous studies, confirming the successful incorporation of silver nanoparticles and their interactions with the PVA polymer[65–71].

The crystal structure properties of the produced nanofibers were investigated through X-ray diffraction (XRD) analyses, and the results are presented in (Fig. 5).

All three Ag-containing nanofiber structures exhibited peaks at 38, 44, 65, and 77° on the 2θ axis. As documented in the literature, the peaks at these values in the XRD patterns correspond to the (111), (200), (220), and (311) crystal planes of the face-centered cubic form of Ag, respectively[56]. In the A1 group, the formation of crystal phases of the AgNPs was observed; however, the peaks remained relatively weak due to the low concentration. This result suggests that a low concentration of silver had a limited effect on the crystal structure. In the 1.0% AgPVA group, the crystalline phases of the AgNPs became more pronounced, and sharper peaks formed. This indicates that the tendency of nanoparticles to crystallize increases with increasing silver concentration, leading to more dominant crystalline phases. The A3 group exhibited the highest density and sharpest peaks, indicating that the AgNPs crystallized in the highest amount and with the best organization. The peak density and clarity demonstrated that, at this concentration, the AgNPs formed the most homogeneous and organized crystal structure. The P10 group displayed an amorphous structure, with no characteristic crystal peaks observed. This observation aligns with the amorphous nature of PVA, which lacks a crystalline structure[72]. The diffuse background noise in the XRD patterns of the PVA-based nanofibers, particularly in the P10 group, can also be attributed to the non-crystalline nature of the polymer matrix. However, the introduction of silver nanoparticles into the PVA matrix (A1, A2, and A3 groups) resulted in the formation of crystalline phases, demonstrating the successful integration of AgNPs. The weak intensity of the peaks in the A1 group, compared to the A2 and A3 groups, may also reflect the heterogeneous distribution of silver nanoparticles at lower concentrations, a phenomenon commonly reported in nanoparticle-polymer systems.

Overall, the findings indicate that increasing silver concentration in the PVA matrix enhances the crystalline characteristics of the nanofibers. Notably, the A3 group contained the most pronounced crystalline phases of the AgNPs, suggesting that AgNPs can be effectively integrated into PVA and that such nanofibers have potential for advanced material applications.

Figure 6 presents SEM images and histograms of nanofiber films containing 10% PVA and various ratios of Ag SEM images, revealed that the nanofibers exhibited a homogeneous, particle-free structure. The average diameter of the nanofibers ranged between 166 and 186 nm. The P10 sample had the largest diameter (186.89 nm) among the samples analyzed via the ImageJ program. Compared with that of the P10 sample, the diameter of the AgPVA nanofibers containing different concentrations of Ag tended to decrease. However, this decrease did not

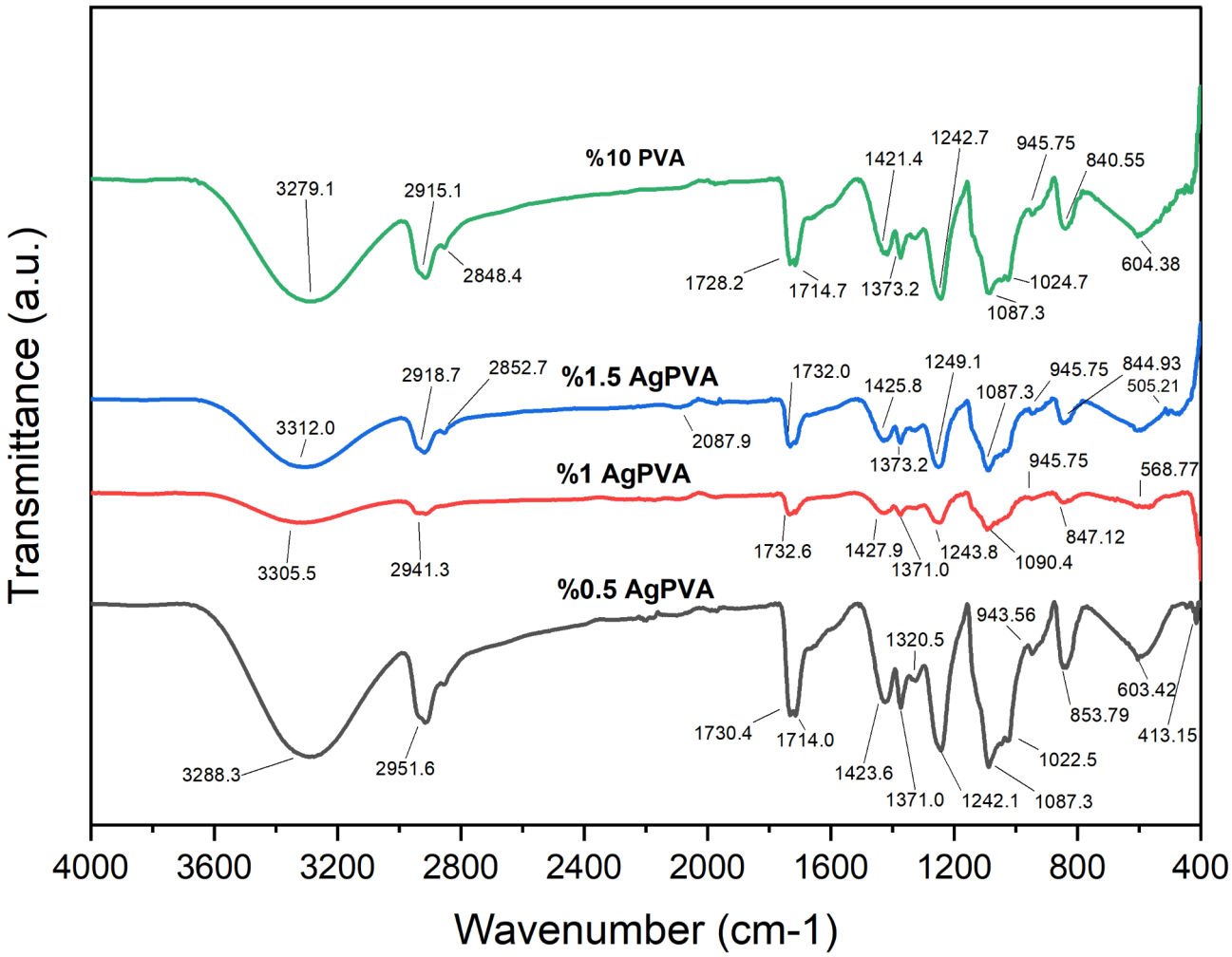

Fig. 4. FT-IR spectra of the AgPVA nanofibers.

significantly differ with respect to the silver concentration. This may suggest that the addition of silver up to a certain concentration has a stabilizing effect on the fiber diameter. It has been reported that AgNPs synthesized from *Ficus altissima* Blume leaf extract produce nanofibers with diameters ranging from 40 nm to 178 nm according to SEM images of a study where AgPVA nanofibers were formed via the electrospinning technique[73].

Figure 7 shows the EDX spectra of the fibers. An analysis of the EDX results revealed that the carbon and oxygen ratios in all the samples confirmed the presence of the PVA polymer. The high proportions of carbon and oxygen indicate the dominance of the polymer matrix. The EDX results show that as the silver concentration increases, the proportion of silver in the nanofibers also increases. However, the difference between the silver ratios in the A2 and A3 groups was not as significant as expected. This is thought to be due to the inhomogeneous distribution of silver particles. In conclusion, silver was successfully integrated into the PVA nanofibers in all the groups, but the differences between the concentrations were less pronounced than expected.

Antibacterial activity of AgPVA nanofibers

The AgPVA nanofibers exhibited substantial inhibitory activity against the tested microorganisms, as presented in (Table 2). A notable difference in the antibacterial effectiveness of the AgPVA nanofibers against pathogenic bacteria was observed with increasing silver concentration (Table 2, $p<0.05$). An increase in the silver concentration resulted in increased antibacterial activity against *Bacillus cereus*, *Staphylococcus aureus*, and *Pseudomonas aeruginosa*, whereas an increased concentration of silver did not significantly affect the inhibition zone for *Escherichia coli*. The AgPVA nanofibers exhibited superior activity (ZOI) against *S. aureus*. Similar results have been reported by[35,50]. The P10 group (nanofibers without AgNPs) exhibited no antibacterial activity, confirming that the antibacterial properties of the AgPVA nanofibers are dependent on the presence of AgNPs on the fiber surface. These results indicate that AgPVA nanofibers possess substantial antibacterial activity against both Gram-positive and Gram-negative microorganisms.

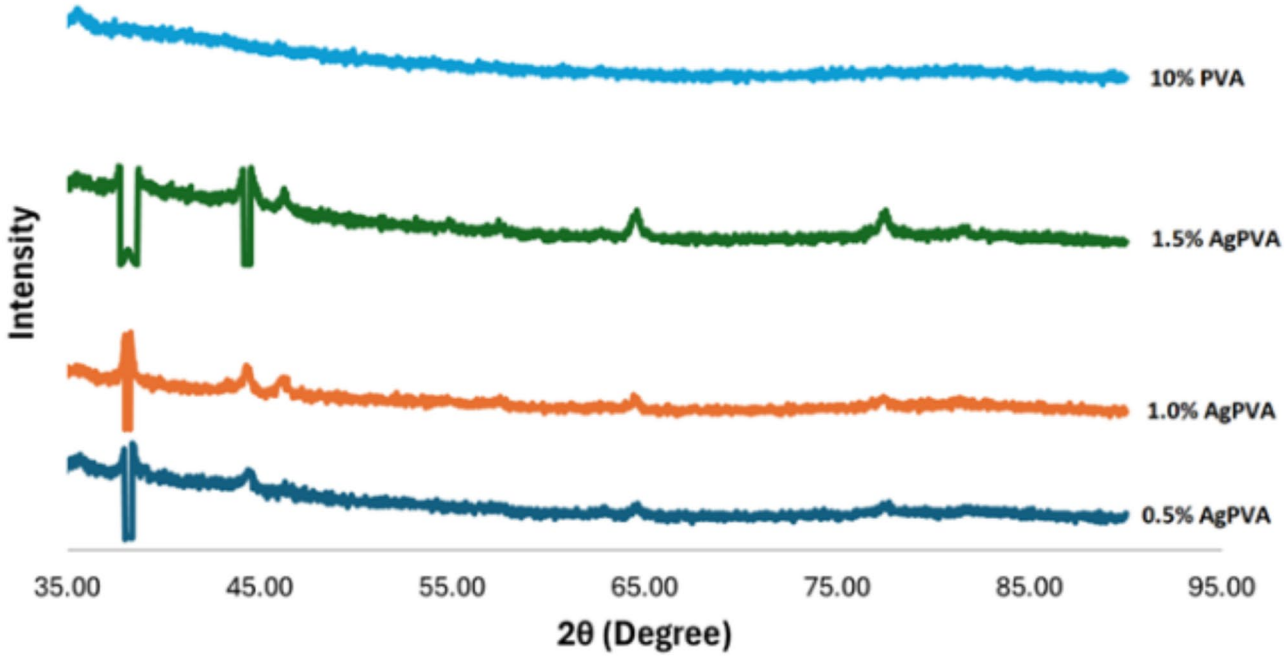

Fig. 5. XRD patterns of the AgPVA nanofibers.

Effects of the AgPVA nanofiber coating on the quality of minced meat

The changes in the pH values of the minced meat during the storage period are presented in (Table 3). Initially, the pH range of fresh minced meat was determined to be 5.87. Compared with the initial pH value, the pH values of all the samples increased significantly ($p < 0.05$). An increase in pH is observed due to the formation of alkaline amines resulting from the breakdown of protein by microorganisms[74]. An increase in the pH of minced meat has also been reported by researchers[75–77]. The pH value of the group containing 0.5% Ag was the lowest during the whole storage period. The results show that the films can reduce the growth of microorganisms, which leads to a lower pH value.

The L* (brightness), a* (redness) and b* (yellowness) values of the minced meat samples are presented in (Table 4). It was determined that the L* values of the minced meat samples with an initial L* value of 51.15 showed a decreasing trend in all groups during the storage period. The highest L* value was observed in 0.5 AgPVA and AgPVA groups in all storage days. The L* value of A1 was the best maintaining the initial level. Day zero a value of minced meat samples was determined as 14.23. A decrease in the a* value of all groups was observed during storage. Until day 6, A1 and A2 group had the highest a* value and no statistical difference was observed between them ($p > 0.0.5$). A3, P10 and NC groups showed a faster decrease in a* value. During storage, A1 group preserved the color (L*, a*, b*) values better than the other groups. This indicates that nanofiber coatings doped with silver at certain concentrations may be effective in preserving the color of minced meat. It was determined that the b* value of the minced meat samples with an initial b* value of 8.85 tended to increase in all groups during the storage period.

The effects of 9 days of storage at 4 °C on the peroxide value (PV) of minced meat samples are presented in (Table 5). The initial PV of all the groups was 2.92 meq O_2/kg fat, measured from the minced meat samples prior to the application of coatings (day 0). PV measurements were subsequently conducted on coated samples at days 3, 6, and 9 to assess the impact of nanofiber coatings during storage. The increase in PV values observed in all groups up to the third day of storage, followed by a subsequent decrease, is likely related to the breakdown of hydroperoxides into secondary oxidation products such as aldehydes, ketones, and hydroxy compounds[78,79]. The highest peroxide value was observed in the NC group throughout the storage period ($p < 0.05$). The A1 and A2 groups presented lower peroxide values after the third day of storage. In various studies, the peroxide value has been reported to range from 2.58 to 5.71 meq O/kg fat in beef patties[80], from 0.84 to 5.63 meq O/kg fat in raw beef hamburgers[81], from 3.31 to 9.73 meq O/kg fat in beef burgers[82], and from 2.11 to 9.65 meq O/kg fat in beef meatballs[83].

Oxidation in meat products is a critical factor in assessing quality, particularly during cold storage. In this context, TBARS values, which represent the secondary products of lipid auto oxidation, are used to determine lipid oxidation in different types of food[40,84]. The TBARS values of the minced meat samples stored for nine days ranged between 0.16 and 1.95 mg MDA/kg (Table 6). The TBARS values increased over time in all the groups, as shown in (Table 6) below. The increase in TBARS values is primarily due to the oxidation of unsaturated fatty acids during storage[85]. During the nine-day storage period, the lowest TBARS value was observed in the AgPVA group, with the A1 group showing a slightly higher value. The findings indicated that the A3 group presented elevated TBARS values throughout the storage period and no statistically significant difference was

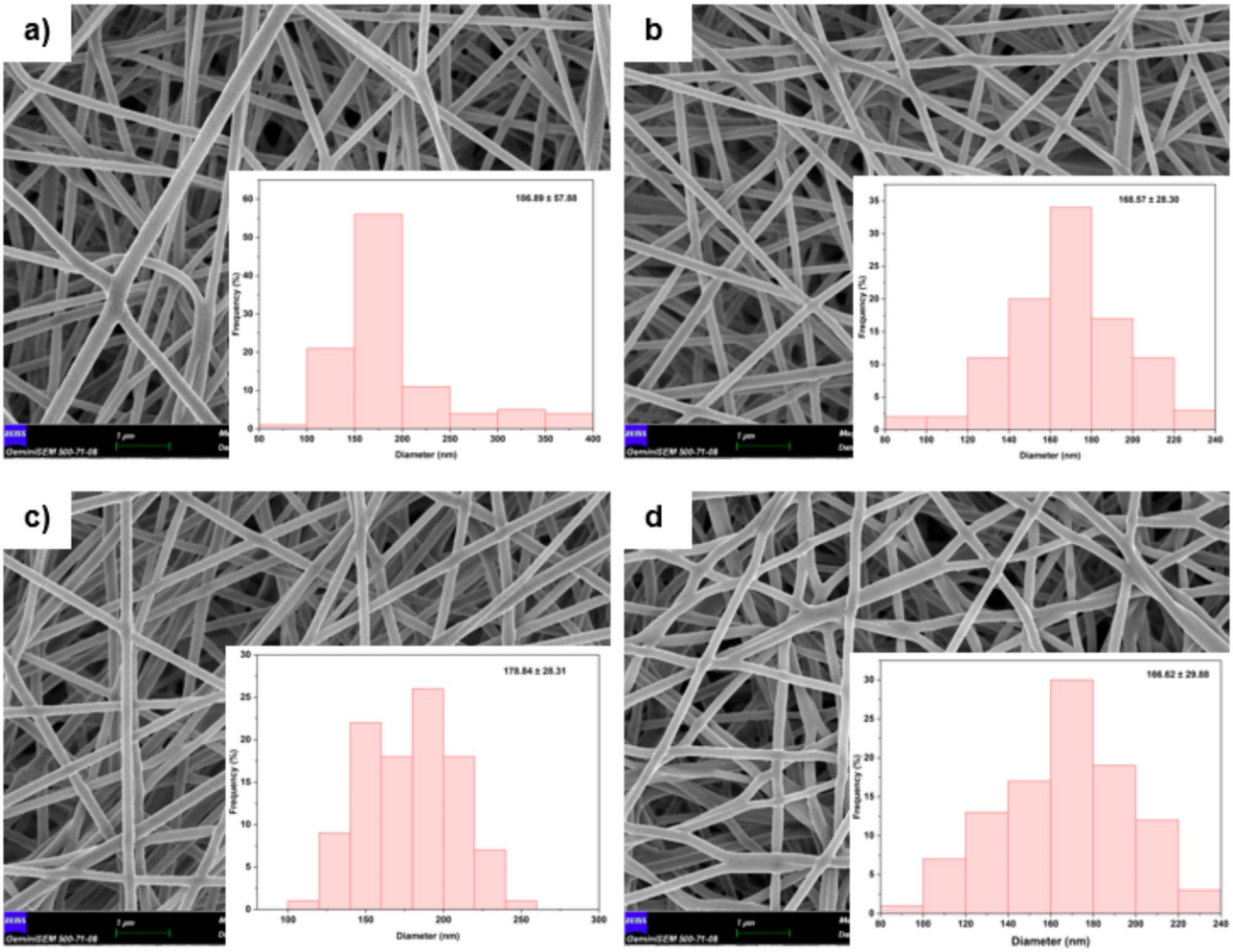

Fig. 6. SEM images of the AgPVA nanofibers. (**a**) Group containing 10% PVA (P10), (**b**) Group containing 0.5% AgPVA (A1), (**c**) Group containing 1.0% AgPVA (A2), (**d**) Group containing 1.5% AgPVA (A3).

detected between this group and the P10 and NC groups on the sixth day ($p > 0.05$). The results suggest that silver concentrations of up to 1.0% can delay the oxidation of minced beef and help preserve its quality.

Researchers have reported initial TBA values of 0.283[86], 0.33[87] and 0.28 mg MDA/kg[88] in studies using beef as a raw material and observed an increase in TBA values throughout the storage period.

Effect of nanofiber treatment on the bacterial counts of minced meat

The effects of nanofiber application on the bacterial counts (TMABc and TPBc) of minced meat samples during storage are shown in (Table 7) below. The initial TMAB load in the minced meat was determined to be 7.43 log CFU/g. The results showed that the total aerobic mesophilic bacteria count exceeded the microbiological criteria of the Turkish Food Codex, which states that the total aerobic mesophilic bacteria count should not exceed 5×10^6 CFU/g (approximately 6.7 log CFU/g). Similar findings have been reported in studies conducted on minced meat products, where microbial loads were observed to be higher due to factors such as inadequate hygiene practices, prolonged storage times, and seasonal conditions. Studies in Türkiye have also highlighted that minced meat often exhibits higher microbial loads due to insufficient hygiene during production and handling[89,90]. Compared with similar studies[40,91,92], the initial load was quite high, but the increase observed during storage was significantly lower in percentage terms than the increases reported in those studies. Compared with the other samples, the sample coated with A1 nanofiber significantly inhibited the growth of TMABc ($p < 0.05$) and provided a notable antimicrobial effect until day 6.

The initial TPBc load of the minced meat samples was determined to be 8.08 log CFU/g. The initial bacterial load of meat products can vary depending on factors such as the slaughter method, storage conditions, and atmospheric hygienic conditions[93]. These findings emphasize the importance of maintaining strict hygiene standards during meat production, processing, and distribution to minimize microbial contamination. As expected, increase in both TMABc and TPBc were observed during the storage period. However, samples coated with A1 and A2 nanofibers showed a significant antimicrobial effect compared with the other groups at the 6-day storage point ($p < 0.05$). On the final day of storage (Day 9), no statistically significant difference was observed in the TMABc and TPBc levels between the samples ($p > 0.05$).

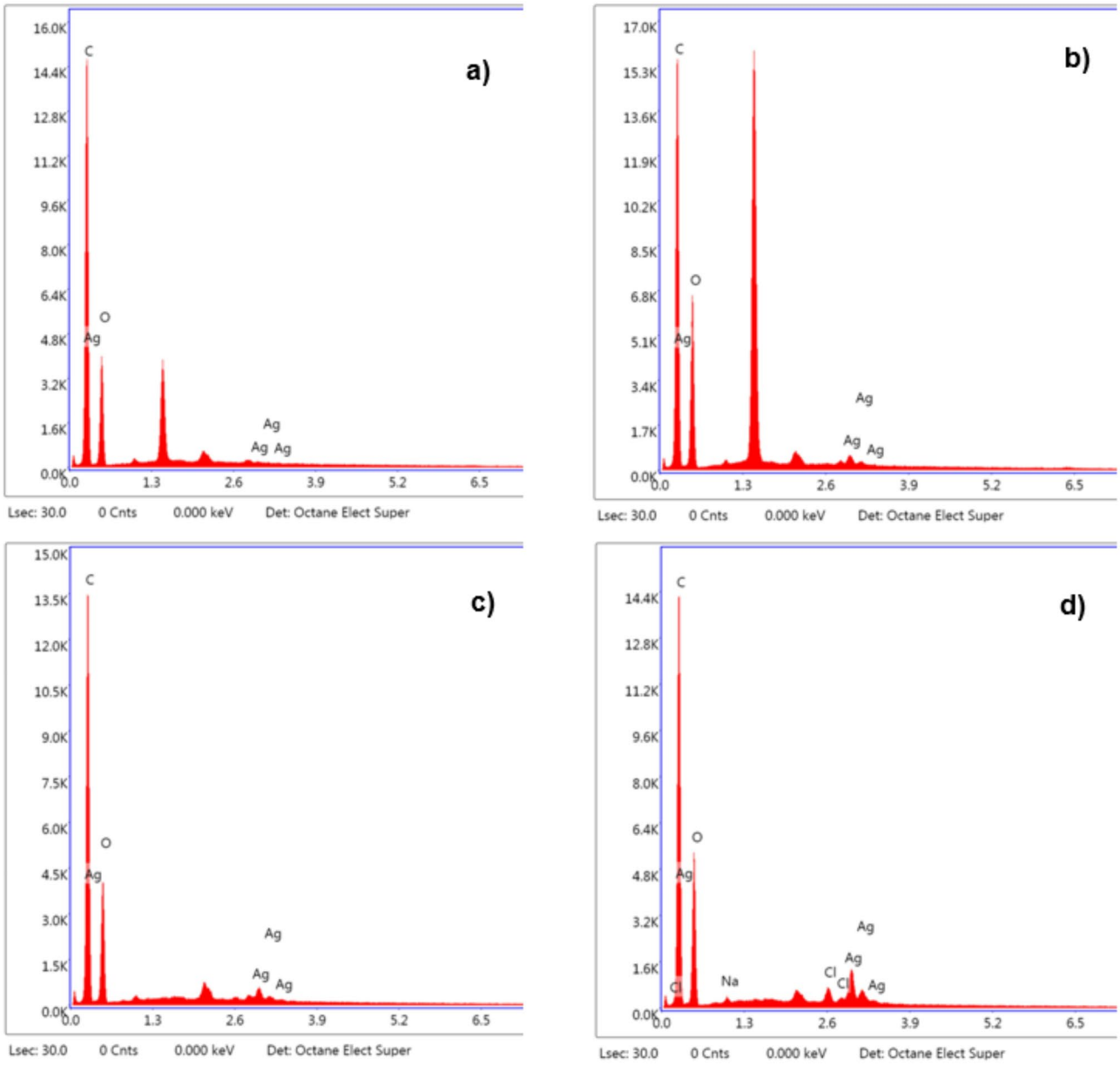

Fig. 7. EDX spectra of the AgPVA nanofibers. (**a**) Group containing 10% PVA (P10), (**b**) Group containing 0.5% AgPVA (A1), (**c**) Group containing 1.0% AgPVA (A2), (**d**) Group containing 1.5% AgPVA (A3).

Bacteria	Zone of the inhibition (mm)				
	Positive control (ampicillin)	Negative control (10% PVA)	0.5% AgPVA	1.0% AgPVA	1.5% AgPVA
B.cereus	$11.95 \pm 0.98^{c, y}$	–	$9.99 \pm 0.17^{b, z}$	$11.03 \pm 0.32^{b, yz}$	$13.95 \pm 0.15^{ab, x}$
S. aureus	$43.06 \pm 1.24^{a, x}$	–	$12.36 \pm 1.07^{ab, z}$	$15.00 \pm 1.77^{a, y}$	$15.44 \pm 1.55^{a, y}$
E.coli	$18.56 \pm 1.11^{b, x}$	–	$14.10 \pm 2.72^{a, y}$	$10.20 \pm 0.15^{b, z}$	$10.12 \pm 1.59^{c, z}$
P. aeruginosa	–	–	$10.79 \pm 0.62^{b, y}$	$11.44 \pm 0.04^{b, xy}$	$12.11 \pm 1.25^{bc, x}$

Table 2. Antibacterial activity of the nanofibers. $^{a-c}$Different letters in the same column indicate a significant difference ($P < 0.05$). The data are presented as the means ± standard errors. $^{x-z}$Different letters in the same row indicate a significant difference ($P < 0.05$). The data are presented as the means ± standard errors.

Storage period (day)				
Samples	**0**	**3**	**6**	**9**
P10	$5.87 \pm 0.01^{a, t}$	$6.15 \pm 0.02^{a, z}$	$6.27 \pm 0.01^{a, y}$	$6.47 \pm 0.08^{a, x}$
A1	$5.87 \pm 0.01^{a, t}$	$6.04 \pm 0.01^{c, z}$	$6.09 \pm 0.01^{d, y}$	$6.20 \pm 0.02^{c, x}$
A2	$5.87 \pm 0.01^{a, t}$	$6.07 \pm 0.01^{b, z}$	$6.12 \pm 0.01^{c, y}$	$6.34 \pm 0.03^{b, x}$
A3	$5.87 \pm 0.01^{a, z}$	$6.10 \pm 0.02^{b, y}$	$6.14 \pm 0.03^{c, y}$	$6.43 \pm 0.12^{ab, x}$
NC	$5.87 \pm 0.01^{a, t}$	$6.15 \pm 0.03^{a, z}$	$6.22 \pm 0.02^{b, y}$	$6.51 \pm 0.04^{a, x}$

Table 3. pH values of minced meat during storage. **P10** PVA nanofibers were prepared at a 10% (w/v) concentration without silver; **A1** AgPVA nanofibers with 0.5% (w/v) Ag; **A2** AgPVA nanofibers with 1.0% (w/v) Ag; **A3** AgPVA nanofibers with 1.5% (w/v) Ag; and NC: aluminum foil without nanofiber film. $^{a–d}$Different letters in the same column indicate a significant difference ($P < 0.05$). The data are presented as the mean ± standard error. $^{x–t}$Different letters in the same row indicate a significant difference ($P < 0.05$). The data are presented as the means ± standard errors.

Samples	Day 0	Day 3	Day 6	Day 9
L*				
P10	$51.15 \pm 0.34^{a, x}$	$44.16 \pm 0.52^{b, y}$	$43.17 \pm 0.43^{b, z}$	$42.55 \pm 0.36^{b, z}$
A1	$51.15 \pm 0.34^{a, x}$	$47.95 \pm 0.44^{a, y}$	$47.00 \pm 0.37^{a, yz}$	$46.45 \pm 1.13^{a, z}$
A2	$51.15 \pm 0.34^{a, x}$	$46.96 \pm 1.64^{a, y}$	$46.04 \pm 1.71^{a, y}$	$45.72 \pm 1.14^{a, y}$
A3	$51.15 \pm 0.34^{a, x}$	$43.41 \pm 1.19^{b, y}$	$41.65 \pm 0.55^{b, z}$	$42.37 \pm 0.55^{b, yz}$
NC	$51.15 \pm 0.34^{a, x}$	$43.59 \pm 0.85^{b, y}$	$42.34 \pm 0.97^{b, yz}$	$41.70 \pm 0.82^{b, z}$
a*				
P10	$14.23 \pm 0.22^{a, x}$	$10.98 \pm 0.16^{b, y}$	$9.67 \pm 0.22^{b, z}$	$8.92 \pm 0.35^{c, t}$
A1	$14.23 \pm 0.22^{a, x}$	$12.62 \pm 0.48^{a, y}$	$11.62 \pm 0.07^{a, z}$	$10.59 \pm 0.40^{b, t}$
A2	$14.23 \pm 0.22^{a, x}$	$13.21 \pm 0.78^{a, y}$	$12.35 \pm 0.24^{a, y}$	$11.32 \pm 0.52^{a, z}$
A3	$14.23 \pm 0.22^{a, x}$	$11.42 \pm 0.45^{b, y}$	$10.37 \pm 0.81^{b, z}$	$9.23 \pm 0.21^{c, t}$
NC	$14.23 \pm 0.22^{a, x}$	$10.92 \pm 0.67^{b, y}$	$9.75 \pm 0.85^{b, z}$	$9.41 \pm 0.15^{c, z}$
b*				
P10	$8.85 \pm 0.01^{a, z}$	$8.97 \pm 0.48^{ab, yz}$	$10.07 \pm 0.33^{a, xy}$	$10.73 \pm 1.10^{a, x}$
A1	$8.85 \pm 0.01^{a, y}$	$8.51 \pm 0.31^{b, y}$	$9.67 \pm 0.06^{ab, x}$	$9.88 \pm 0.36^{a, x}$
A2	$8.85 \pm 0.01^{a, z}$	$9.33 \pm 0.29^{a, yz}$	$9.88 \pm 0.55^{a, xy}$	$10.10 \pm 0.36^{a, x}$
A3	$8.85 \pm 0.01^{a, y}$	$8.72 \pm 0.44^{ab, y}$	$8.81 \pm 0.46^{b, y}$	$9.81 \pm 0.18^{a, x}$
NC	$8.85 \pm 0.01^{a, yz}$	$8.40 \pm 0.09^{b, y}$	$9.78 \pm 0.86^{ab, y}$	$10.92 \pm 0.62^{a, x}$

Table 4. Color values (L* a* b*) of minced meat during storage. **P10** PVA nanofibers were prepared at a 10% (w/v) concentration without silver; **A1** AgPVA nanofibers with 0.5% (w/v) Ag; **A2** AgPVA nanofibers with 1.0% (w/v) Ag; **A3** AgPVA nanofibers with 1.5% (w/v) Ag; and NC: aluminum foil without nanofiber film. $^{a–c}$Different letters in the same column indicate a significant difference ($P < 0.05$). The data are presented as the means ± standard errors. $^{x–t}$Different letters in the same row indicate a significant difference ($P < 0.05$). The data are presented as the means ± standard errors.

Our findings are consistent with previous studies in the literature. Researchers have reported that silver nanoparticle-based coatings effectively inhibit the growth of spoilage microorganisms in meat products[12,14,15,18,94].

Migration of silver test

The migration of AgNPs into minced meat samples was monitored over 3, 6, and 9 days of storage, and the results are presented in (Fig. 8). The migration levels were dependent on the concentration of AgNPs in the coatings, with the A3 group exhibiting the highest migration value of 0.023 mg/kg on day 3. However, all migration values recorded for the A1, A2, and A3 groups remained well below the European Food Safety Authority (EFSA) safety limit of 0.05 mg/kg for silver migration into food[95]. This demonstrates that the AgNP-based coatings provide a safe and effective means of controlling microbial growth without posing significant migration risks.

AgNPs are widely recognized for their antimicrobial properties, which make them suitable for food preservation. However, uncontrolled migration of silver into food can pose health risks due to its potential toxicity[20]. Studies investigating the migration behavior of AgNP-based films in food systems have reported varying outcomes depending on the film composition and storage conditions. For instance, one study reported that biologically synthesized AgNP films exhibited migration values exceeding EFSA's limits (12.94 mg/kg and 3.79 mg/kg) when applied to chicken meat[22]. In contrast, research on PLA-based nanocomposite films demonstrated that migration levels remained within acceptable limits for food simulant[21]. Similarly, another

Peroxide value (meqO_2/kg)				
Samples	**Day 0**	**Day 3**	**Day 6**	**Day 9**
P10	$2.92 \pm 0.92^{a, y}$	$8.71 \pm 2.17^{bc, x}$	$5.05 \pm 0.49^{bc, y}$	$5.41 \pm 1.24^{ab, y}$
A1	$2.92 \pm 0.92^{a, z}$	$9.44 \pm 0.57^{ab, x}$	$4.93 \pm 0.12^{bc, y}$	$4.70 \pm 0.67^{b, y}$
A2	$2.92 \pm 0.92^{a, y}$	$7.53 \pm 1.23^{bc, x}$	$4.51 \pm 0.93^{c, y}$	$4.70 \pm 0.38^{b, y}$
A3	$2.92 \pm 0.92^{a, z}$	$6.72 \pm 0.59^{c, x}$	$5.72 \pm 0.26^{b, xy}$	$5.33 \pm 0.30^{ab, y}$
NC	$2.92 \pm 0.92^{a, z}$	$11.46 \pm 0.95^{a, x}$	$7.23 \pm 0.48^{a, y}$	$6.49 \pm 0.11^{a, y}$

Table 5. Peroxide values of minced meat during storage. **P10** PVA nanofibers prepared at a 10% (w/v) concentration without silver; **A1** AgPVA nanofibers with 0.5% (w/v) Ag; **A2** AgPVA nanofibers with 1.0% (w/v) Ag; **A3** AgPVA nanofibers with 1.5% (w/v) Ag; and NC: aluminum foil without nanofiber film. $^{a-c}$Different letters in the same column indicate a significant difference ($P < 0.05$). The data are presented as the means ± standard errors. $^{x-z}$Different letters in the same row indicate a significant difference ($P < 0.05$). The data are presented as the means ± standard errors.

TBARS values (mg MDA/kg)				
Samples	**Day 0**	**Day 3**	**Day 6**	**Day 9**
P10	$0.159 \pm 0.003^{a, z}$	$0.283 \pm 0.011^{a, y}$	$0.284 \pm 0.008^{a, y}$	$1.886 \pm 0.016^{b, x}$
A1	$0.159 \pm 0.003^{a, t}$	$0.191 \pm 0.008^{d, z}$	$0.239 \pm 0.014^{b, y}$	$0.912 \pm 0.026^{c, x}$
A2	$0.159 \pm 0003^{a, z}$	$0.161 \pm 0.005^{e, z}$	$0.217 \pm 0.008^{c, y}$	$0.510 \pm 0.046^{d, x}$
A3	$0.159 \pm 0.003^{a, t}$	$0.211 \pm 0.008^{c, z}$	$0.274 \pm 0.003^{a, y}$	$1.877 \pm 0.005^{b, x}$
NC	$0.159 \pm 0.003^{a, t}$	$0.258 \pm 0.008^{b, z}$	$0.288 \pm 0.008^{a, y}$	$1.947 \pm 0.021^{a, x}$

Table 6. TBARS values of minced meat during storage. **P10** PVA nanofibers prepared at a 10% (w/v) concentration without silver; **A1** AgPVA nanofibers with 0.5% (w/v) Ag; **A2** AgPVA nanofibers with 1.0% (w/v) Ag; **A3** AgPVA nanofibers with 1.5% (w/v) Ag; and NC: aluminum foil without nanofiber film. $^{a-e}$Different letters in the same column indicate a significant difference ($P < 0.05$). The data are presented as the means ± standard errors. $^{x-t}$Different letters in the same row indicate a significant difference ($P < 0.05$). The data are presented as the means ± standard errors.

Samples	**Day 0**	**Day 3**	**Day 6**	**Day 9**
TMABc (log cfu/g)				
P10	$7.43 \pm 0.18^{a, t}$	$8.34 \pm 0.41^{ab, z}$	$9.08 \pm 0.07^{a, y}$	$9.43 \pm 0.52^{a, x}$
A1	$7.43 \pm 0.18^{a, z}$	$7.57 \pm 0.17^{c, z}$	$8.45 \pm 0.13^{b, y}$	$8.94 \pm 0.35^{a, x}$
A2	$7.43 \pm 0.18^{a, t}$	$7.87 \pm 0.30^{bc, z}$	$9.10 \pm 0.09^{a, y}$	$9.30 \pm 0.28^{a, x}$
A3	$7.43 \pm 0.18^{a, y}$	$8.53 \pm 0.53^{a, x}$	$8.97 \pm 0.17^{a, x}$	$9.14 \pm 0.44^{a, x}$
NC	$7.43 \pm 0.18^{a, t}$	$8.56 \pm 0.09^{a, z}$	$9.08 \pm 0.43^{a, y}$	$9.46 \pm 0.18^{a, x}$
TPBc (log cfu/g)				
P10	$8.08 \pm 0.17^{a, y}$	$9.16 \pm 0.03^{a, x}$	$9.61 \pm 0.20^{ab, x}$	$10.26 \pm 1.10^{a, x}$
A1	$8.08 \pm 0.17^{a, y}$	$8.25 \pm 0.02^{b, y}$	$9.40 \pm 0.39^{bc, x}$	$9.70 \pm 0.46^{a, x}$
A2	$8.08 \pm 0.17^{a, y}$	$8.24 \pm 0.14^{b, y}$	$8.95 \pm 0.39^{c, x}$	$9.11 \pm 0.48^{a, x}$
A3	$8.08 \pm 0.17^{a, z}$	$9.19 \pm 0.01^{a, y}$	$9.62 \pm 0.31^{ab, xy}$	$10.26 \pm 0.91^{a, x}$
NC	$8.08 \pm 0.17^{a, z}$	$9.17 \pm 0.03^{a, y}$	$10.19 \pm 0.29^{a, x}$	$10.27 \pm 0.43^{a, x}$

Table 7. Effects of nanofiber treatment on the bacterial counts of minced meat during storage. **P10** PVA nanofibers prepared at a 10% (w/v) concentration without silver; **A1** AgPVA nanofibers with 0.5% (w/v) Ag; **A2** AgPVA nanofibers with 1.0% (w/v) Ag; **A3** AgPVA nanofibers with 1.5% (w/v) Ag; and NC: aluminum foil without nanofiber film. $^{a-c}$Different letters in the same column indicate a significant difference ($P < 0.05$). The data are presented as the means ± standard errors. $^{x-t}$Different letters in the same row indicate a significant difference ($P < 0.05$). The data are presented as the means ± standard errors.

study found that green-synthesized AgNP films derived from dragon fruit stem were safe for short-term storage applications, such as strawberry preservation[96]. Moreover, biodegradable AgNP-containing films were shown to be safe for preserving fresh apple slices for up to five days[20], while gradual increases in silver content were observed over seven days in strawberries coated with PLA films containing green-synthesized AgNPs from mango peel, though the migration levels remained within standard limits[97].

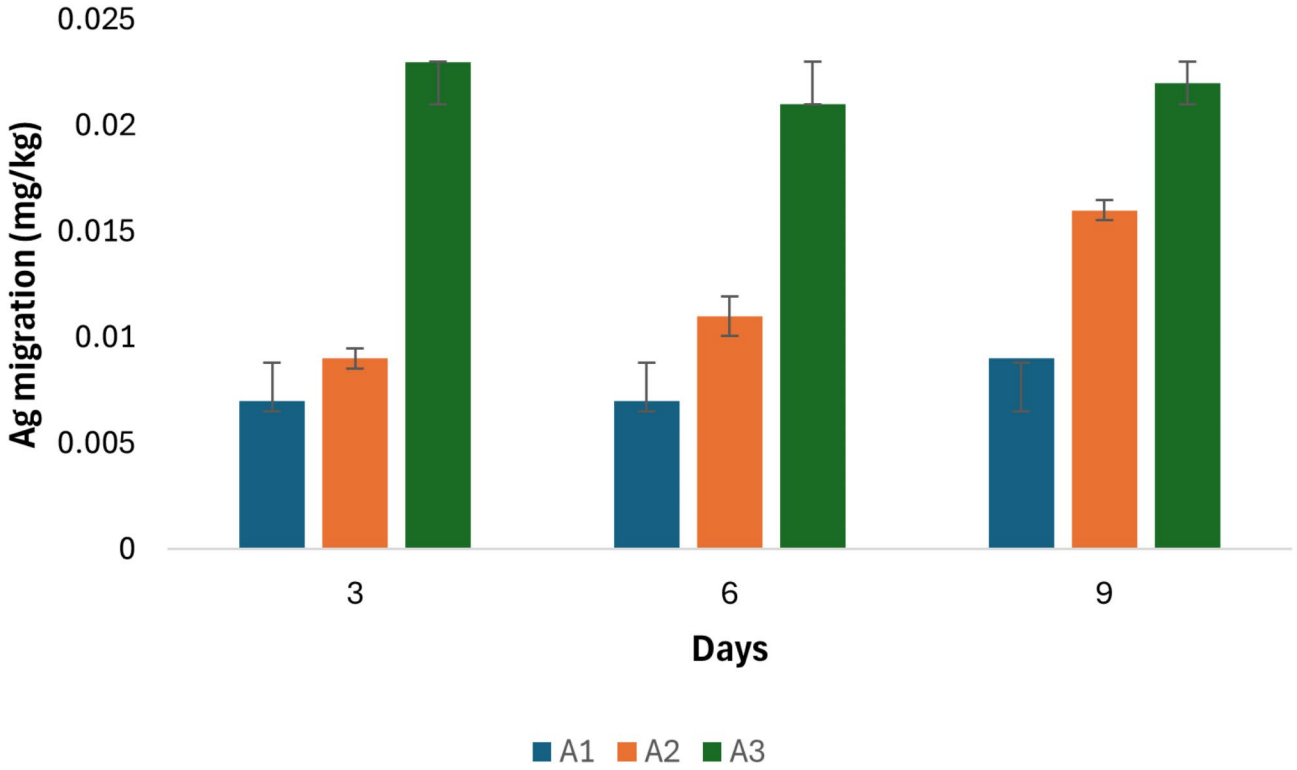

Fig. 8. Migration of Ag from AgPVA nanofiber coatings into minced meat.

Conclusion

In this study, AgNPs were successfully synthesized via the use of pomegranate peel extract, and silver polyvinyl alcohol (AgPVA) nanofibres were fabricated by electrospinning for potential application in food packaging. The successful synthesis of the AgNPs and the homogeneity of the nanofiber structure were confirmed via characterisation analyses. The antibacterial activity of AgNPs was evaluated against both Gram-positive and Gram-negative bacteria, and the greatest inhibitory effects were observed against *Staphylococcus aureus* and *Pseudomonas aeruginosa*. These findings indicated that elevated concentrations of AgNPs were associated with enhanced antibacterial efficacy. The A1 nanofiber group presented the most stable pH values and the highest L* values when it was applied to minced meat, thereby maintaining the color quality of the meat throughout storage. Compared with the control samples, the A1 and A2 groups presented effective reductions in peroxide values and delayed lipid oxidation. These findings indicate that silver concentrations of up to 1% can assist in maintaining meat quality by slowing down oxidation processes. Moreover, samples coated with A1 exhibited a notable decline in microbial growth (TMABc) until day 6 of storage. Additionally, migration analyses revealed that the migration levels of AgNPs from the nanofiber coatings into minced meat samples remained within the European Food Safety Authority (EFSA) safety limit of 0.05 mg/kg throughout the storage period. In conclusion, the results demonstrate that AgPVA nanofibers, particularly those containing 0.5% Ag, have significant potential as antimicrobial coating materials to extend the shelf life of perishable foods, delay spoilage and maintain quality. Further research could investigate the optimization of nanoparticle concentrations and the scaling up of production for wider applications in food coatings.

Data availability

All data analysed during this study are included in this published article.

Received: 18 October 2024; Accepted: 20 March 2025
Published online: 16 May 2025

References

1. Zhan, F., Yan, X., Sheng, F. & Li, B. Facile in situ synthesis of silver nanoparticles on tannic acid/zein electrospun membranes and their antibacterial, catalytic and antioxidant activities. *Food Chem.* **330**, (2020).
2. Ashok, B., Hariram, N., Siengchin, S. & Rajulu, A. V. Modification of tamarind fruit shell powder with in situ generated copper nanoparticles by single step hydrothermal method. *J. Bioresour. Bioprod.* **5**, 180–185 (2020).
3. De Pereira, D. A. & Cruz, J. M. Paseiro Losada, P. Active and intelligent packaging for the food industry. *Food Rev. Int.* **28**, 146–187 (2012).
4. Suppakul, P., Miltz, J., Sonneveld, K. & Bigger, S. W. Active packaging technologies with an emphasis on antimicrobial packaging and its applications. *J. Food Sci.* **68**, 408–420 (2003).

5. Calva-Estrada, S. J., Jiménez-Fernández, M. & Lugo-Cervantes, E. Protein-based films: advances in the development of biomaterials applicable to food packaging. *Food Eng. Rev.* **11**, 78–92 (2019).
6. Fabra, M. J., López-Rubio, A. & Lagaron, J. M. Use of the electrohydrodynamic process to develop active/bioactive bilayer films for food packaging applications. *Food Hydrocoll.* **55**, 11–18 (2016).
7. Montazer, M. & Harifi, T. 16 - New approaches and future aspects of antibacterial food packaging: from nanoparticles coating to nanofibers and nanocomposites, with foresight to address the regulatory uncertainty. in *Food Packaging* (ed. Grumezescu, A. M.) 533–565 https://doi.org/10.1016/B978-0-12-804302-8.00016-9 (Academic Press, 2017).
8. Zhang, W. & Jiang, W. Antioxidant and antibacterial Chitosan film with tea polyphenols-mediated green synthesis silver nanoparticle via a novel one-pot method. *Int. J. Biol. Macromol.* **155**, 1252–1261 (2020).
9. Kochkina, N. E. & Butikova, O. A. Effect of fibrous TiO_2 filler on the structural, mechanical, barrier and optical characteristics of biodegradable maize starch/pva composite films. *Int. J. Biol. Macromol.* **139**, 431–439 (2019).
10. Roy, S. & Rhim, J. W. Carboxymethyl cellulose-based antioxidant and antimicrobial active packaging film incorporated with Curcumin and zinc oxide. *Int. J. Biol. Macromol.* **148**, 666–676 (2020).
11. Zhang, W., Roy, S. & Rhim, J. Copper-based nanoparticles for biopolymer-based functional films in food packaging applications. *Comp. Rev. Food Sci. Food Safe* **22**, 1933–1952 (2023).
12. Carbone, M., Donia, D. T., Sabbatella, G. & Antiochia, R. Silver nanoparticles in polymeric matrices for fresh food packaging. *J. King. Saud. Univ. Sci.* **28**, 273–279 (2016).
13. Mohamed, J. M. M. et al. Superfast synthesis of stabilized silver nanoparticles using aqueous allium sativum (garlic) extract and Isoniazid Hydrazide conjugates: molecular Docking and in-vitro characterizations. *Molecules* **27**, 110 (2021).
14. Mahdi, S. S., Vadood, R. & Nourdahr, R. Study on the antimicrobial effect of nanosilver tray packaging of minced beef at refrigerator temperature. (2012).
15. Martínez-Abad, A., Lagaron, J. M. & Ocio, M. J. Development and characterization of silver-based antimicrobial ethylene–vinyl alcohol copolymer (EVOH) films for food-packaging applications. *J. Agric. Food Chem.* **60**, 5350–5359 (2012).
16. Metak, A. M. Effects of nanocomposite based nano-silver and nano-titanium dioxide on food packaging materials. *Int. J. Appl. Sci. Technol.* **5**, 26–40 (2015).
17. Valipoor Motlagh, N., Hamed Mosavian, M. T. & Mortazavi, S. A. Effect of polyethylene packaging modified with silver particles on the microbial, sensory and appearance of dried barberry. *Packag. Technol. Sci.* **26**, 39–49 (2013).
18. Badawy, M. E. I., Lotfy, T. M. R. & Shawir, S. M. S. Preparation and antibacterial activity of chitosan-silver nanoparticles for application in preservation of minced meat. *Bull. Natl. Res. Cent.* **43**, 83 (2019).
19. Atta, O. M. et al. Silver decorated bacterial cellulose nanocomposites as antimicrobial food packaging materials. *ES Food Agrofor.* **6**, 12–26 (2021).
20. Mouzahim, M. E. et al. Effect of Kaolin clay and ficus carica mediated silver nanoparticles on Chitosan food packaging film for fresh Apple slice preservation. *Food Chem.* **410**, 135470 (2023).
21. Li, W. et al. Development of antimicrobial packaging film made from Poly (lactic acid) incorporating titanium dioxide and silver nanoparticles. *Molecules* **22**, 1170 (2017).
22. da das Neves, M. Antibacterial activity of biodegradable films incorporated with biologically-synthesized silver nanoparticles and the evaluation of their migration to chicken meat. *Antibiotics* **12**, 178 (2023).
23. Abdelhamid, A. E., Yousif, E. A. A. & El-Saidi, M. M. T. El-Sayed, A. A. Polyvinyl alcohol food packaging system comprising green synthesized silver nanoparticles. *Indonesian J. Chem.* **21**, 350–360 (2020).
24. Teixeira, M. A., Amorim, M. T. P. & Felgueiras, H. P. Poly (vinyl alcohol)-based nanofibrous electrospun scaffolds for tissue engineering applications. *Polymers* **12**, 7 (2019).
25. Teodorescu, M., Bercea, M. & Morariu, S. Biomaterials of Poly(vinyl alcohol) and natural polymers. *Polym. Rev.* **58**, 247–287 (2018).
26. Türkoğlu, G. C. et al. PVA-based electrospun materials—A promising route to designing nanofiber Mats with desired morphological shape—A review. *Int. J. Mol. Sci.* **25**, 1668 (2024).
27. Yontar, A. K. & Çevik, S. Effects of plant extracts and green-synthesized silver nanoparticles on the Polyvinyl alcohol (PVA) nanocomposite films. *Arab. J. Sci. Eng.* **48**, 12043–12060 (2023).
28. Nasiriboroumand, M., Montazer, M. & Barani, H. Preparation and characterization of biocompatible silver nanoparticles using pomegranate peel extract. *J. Photochem. Photobiol., B* **179**, 98–104 (2018).
29. Gullón, P., Astray, G., Gullón, B., Tomasevic, I. & Lorenzo, J. M. Pomegranate Peel as suitable source of high-added value bioactives: tailored functionalized meat products. *Molecules* **25**, 2859 (2020).
30. Gopalakrishnan, K. et al. Valorisation of fruit Peel bioactive into green synthesized silver nanoparticles to modify cellulose wrapper for shelf-life extension of packaged bread. *Food Res. Int.* **164**, 112321 (2023).
31. Wang, W. et al. One-step synthesis of biocompatible gold nanoparticles using Gallic acid in the presence of poly-(*N*-vinyl-2-pyrrolidone). *Coll. Surf. A* **301**, 73–79 (2007).
32. Suhag, R. et al. Fruit Peel bioactives, valorisation into nanoparticles and potential applications: A review. *Crit. Rev. Food Sci. Nutr.* **63**, 6757–6776 (2023).
33. Lončarić, A. et al. Peel of traditional Apple varieties as a great source of bioactive compounds: extraction by micro-matrix solid-phase dispersion. *Foods* **9**, 80 (2020).
34. Zia, S., Khan, M. R., Mousavi Khaneghah, A. & Aadil, R. M. Characterization, bioactive compounds, and antioxidant profiling of edible and waste parts of different watermelon (Citrullus lanatus) cultivars. *Biomass Convers. Biorefinery*. 1–13. https://doi.org/10.1007/s13399-023-04820-7 (2023).
35. Kowsalya, E., MosaChristas, K., Balashanmugam, P. & Rani, J. C. Biocompatible silver nanoparticles/poly (vinyl alcohol) electrospun nanofibers for potential antimicrobial food packaging applications. *Food Packag. Shelf Life* **21**, 100379 (2019).
36. Pawar, A. A. et al. Azadirachta indica -derived silver nanoparticle synthesis and its antimicrobial applications. *J. Nanomater.* 4251229 (2022).
37. Sharma, N. K. et al. Green route synthesis and characterization techniques of silver nanoparticles and their biological adeptness. *ACS Omega* **7**, 27004–27020 (2022).
38. Koniecko, E. S. Handbook for meat chemists. (1979).
39. Witte, V. C., Krause, G. F. & Bailey, M. E. A new extraction method for determining 2-thiobarbituric acid values of pork and beef during storage. *J. Food Sci.* **35**, 582–585 (1970).
40. Ceylan, Z. et al. A novel material for the Microbiological, oxidative, and color stability of salmon and chicken meat samples: nanofibers obtained from Sesame oil. *Food Res. Int.* **170**, 112952 (2023).
41. Sabzevar, A. H., Aflakian, F. & Hashemitabar, G. Characterization and evaluation of antibacterial, antioxidant and cytotoxic activities of green synthesized silver nanoparticles using *Haloxylon persicum*. *J. Mol. Struct.* **1304**, 137615 (2024).
42. Du, P. et al. Preparation and shape change of silver nanoparticles (AgNPs) loaded on the dialdehyde cellulose by in-situ synthesis method. *Cellulose* **29**, 6831–6843 (2022).
43. Kota, S., Dumpala, P., Anantha, R. K., Verma, M. K. & Kandepu, S. Evaluation of therapeutic potential of the silver/silver chloride nanoparticles synthesized with the aqueous leaf extract of Rumex acetosa. *Sci. Rep.* **7**, 11566 (2017).
44. Mačák, L. et al. Preparation of green silver nanoparticles and eco-friendly polymer–AgNPs nanocomposites: A study of toxic properties across multiple organisms. *Polymers* **16**, 1865 (2024).

45. Serdar, G. Green biosynthesis of silver nanoparticles were obtained from the extract of pomegranate (*Punica granatum* L.) leaves by supercritical extraction using microwave method. *Celal Bayar Univ. J. Sci.* **19**, 351–358 (2023).
46. Thilagavathi, T., Renuka, R. & Priya, R. S. Bio-Synthesis of silver nanoparticles using *Punica granatum* (pomegranate) Peel extract: A novel approach towards waste utilization. *Int. J. Adv. Sci. Eng.* **3**, 234–236 (2016).
47. Farouk, S. M. et al. Biosynthesis and characterization of silver nanoparticles from *Punica granatum* (pomegranate) Peel waste and its application to inhibit foodborne pathogens. *Sci. Rep.* **13**, 19469 (2023).
48. Joshi, S. J., Geetha, S. J., Al-Mamari, S. & Al-Azkawi, A. Green synthesis of silver nanoparticles using pomegranate Peel extracts and its application in photocatalytic degradation of methylene blue. *Jundishapur. J. Nat. Pharm. Prod.* **13**, (2018).
49. Parhizkar, N., Shahrabi, T. & Ramezanzadeh, B. Steel surface pre-treated by an advance and eco-friendly cerium oxide nanofilm modified by graphene oxide nanosheets; electrochemical and adhesion measurements. *J. Alloys Compd.* **747**, 109–123 (2018).
50. Zhang, Z. et al. Fabrication of silver nanoparticles embedded into Polyvinyl alcohol (Ag/PVA) composite nanofibrous films through electrospinning for antibacterial and surface-enhanced Raman scattering (SERS) activities. *Mater. Sci. Eng. C* **69**, 462–469 (2016).
51. Ramesh, S., Leen, K. H., Kumutha, K. & Arof, A. K. FTIR studies of PVC/PMMA blend based polymer electrolytes. *Spectrochim. Acta Part A Mol. Biomol. Spectrosc.* **66**, 1237–1242 (2007).
52. Sofi, H. S. et al. Novel lavender oil and silver nanoparticles simultaneously loaded onto polyurethane nanofibers for wound-healing applications. *Int. J. Pharm.* **569**, 118590 (2019).
53. Dzimitrowicz, A. et al. Comparison of the characteristics of gold nanoparticles synthesized using aqueous plant extracts and natural plant essential oils of *Eucalyptus globulus* and *Rosmarinus officinalis*. *Arab. J. Chem.* **12**, 4795–4805 (2019).
54. Ghaedi, M., Yousefinejad, M., Safarpoor, M., Khafri, H. Z. & Purkait, M. K. Rosmarinus officinalis leaf extract mediated green synthesis of silver nanoparticles and investigation of its antimicrobial properties. *J. Ind. Eng. Chem.* **31**, 167–172 (2015).
55. Predoi, D. et al. Properties of Basil and lavender essential oils adsorbed on the surface of hydroxyapatite. *Materials* **11**, 652 (2018).
56. Wang, S., Bai, J., Li, C., Zhang, Y. & Zhang, J. Ag nanoparticle-embedded one-dimensional β-CD/PVP composite nanofibers prepared via electrospinning for use in antibacterial material. *Coll. Polym. Sci.* **290**, 667–672 (2012).
57. Mafhala, L. et al. Antibacterial and cytotoxicity activity of green synthesized silver nanoparticles using aqueous extract of Naartjie (*Citrus unshiu)* fruit peels. *Emerg. Contaminants* **10**, 100348 (2024).
58. Aslany, S., Tafvizi, F. & Naseh, V. Characterization and evaluation of cytotoxic and apoptotic effects of green synthesis of silver nanoparticles using *Artemisia ciniformis* on human gastric adenocarcinoma. *Mater. Today Commun.* **24**, 101011 (2020).
59. Hazman, Ö. et al. Green synthesis of ag nanoparticles from Verbascum insulare Boiss. and Heldr.: evaluation of antimicrobial, anticancer, antioxidant properties And photocatalytic degradation of MB. *J. Photochem. Photobiol. A* **453**, 115601 (2024).
60. Mousavi, B., Tafvizi, F. & Zaker Bostanabad, S. Green synthesis of silver nanoparticles using *Artemisia turcomanica* leaf extract and the study of anti-cancer effect and apoptosis induction on gastric cancer cell line (AGS). *Artif. Cells Nanomed. Biotechnol.* **46**, 499–510 (2018).
61. More, P. R. et al. Silver nanoparticles: bactericidal and mechanistic approach against drug resistant pathogens. *Microorganisms* **11**, 369 (2023).
62. Agnihotri, S., Mukherji, S. & Mukherji, S. Size-controlled silver nanoparticles synthesized over the range 5–100 Nm using the same protocol and their antibacterial efficacy. *RSC Adv.* **4**, 3974–3983 (2014).
63. Hashemitabar, G., Aflakian, F. & Sabzevar, A. H. Assessment of antibacterial, antioxidant, and anticancer effects of biosynthesized silver nanoparticles using *Teucrium polium* extract. *J. Mol. Struct.* **1291**, 136076 (2023).
64. Ahmad, S. A. et al. Bactericidal activity of silver nanoparticles: A mechanistic review. *Mater. Sci. Energy Technol.* **3**, 756–769 (2020).
65. Chellamani, K. P., Sundaramoorthy, P. & Sureshram, T. Characterisation of Poly vinyl alcohol (PVA)/Silver nitrate nanomembranes for their suitability in wound dressing applications. *Int. J. Emerg. Technol. Adv. Eng.* **2**, 176–184 (2012).
66. Ilčin, M., Holá, O., Bakajová, B. & Kučerík, J. FT-IR study of gamma-radiation induced degradation of Polyvinyl alcohol (PVA) and PVA/humic acids blends. *J. Radioanal. Nucl. Chem.* **283**, 9–13 (2010).
67. Jyoti, K., Baunthiyal, M. & Singh, A. Characterization of silver nanoparticles synthesized using urtica dioica Linn. Leaves and their synergistic effects with antibiotics. *J. Radiat. Res. Appl. Sci.* **9**, 217–227 (2016).
68. Mansur, H. S., Sadahira, C. M., Souza, A. N. & Mansur, A. A. P. FTIR spectroscopy characterization of Poly (vinyl alcohol) hydrogel with different hydrolysis degree and chemically crosslinked with glutaraldehyde. *Mater. Sci. Eng. C* **28**, 539–548 (2008).
69. Nguyen, T., Kim, Y., Song, H. & Lee, B. Nano ag loaded PVA nano-fibrous Mats for skin applications. *J. Biomed. Mater. Res.* **96B**, 225–233 (2011).
70. Slistan-Grijalva, A. et al. Synthesis of silver nanoparticles in a polyvinylpyrrolidone (PVP) paste, and their optical properties in a film and in ethylene glycol. *Mater. Res. Bull.* **43**, 90–96 (2008).
71. Sunaryono, S. et al. The effect of ag nanoparticles in ag/polyvinyl alcohol nanofiber composites. *Polym. Bull.* **79**, 555–568 (2022).
72. Kavgacı, M. & Eskalen, H. Morphology, structure and optical properties of PVA nanocomposites reinforced with bismuth oxide nanoparticles and carbon quantum Dots. *J. Mater. Sci. Mater. Electron.* **34**, 1229 (2023).
73. Meng, Y. A sustainable approach to fabricating ag nanoparticles/pva hybrid nanofiber and its catalytic activity. *Nanomaterials* **5**, 1124–1135 (2015).
74. Naeeji, N., Shahbazi, Y. & Shavisi, N. Effect of gamma irradiation on physico-mechanical and structural properties of Basil seed mucilage-chitosan films containing *Ziziphora clinopodioides* essential oil and MgO nanoparticles for rainbow trout packaging. *J. Food Process. Preserv.* **44**, (2020).
75. Abdin, M. et al. Production of novel bio-transfer films composed from Polyvinyl alcohol/sodium caseinate enhanced with bonded anthocyanins from poinsettia for minced meat preservation in double sheet system. *Food Meas.* **18**, 6956–6972 (2024).
76. Goudarzi, J., Moshtaghi, H. & Shahbazi, Y. Kappa-carrageenan-poly(vinyl alcohol) electrospun fiber Mats encapsulated with *Prunus domestica* anthocyanins and Epigallocatechin gallate to monitor the freshness and enhance the shelf-life quality of minced beef meat. *Food Packag. Shelf Life* **35**, 101017 (2023).
77. Zhao, J. et al. Application of Ag@SiO_2 nanoparticles within PVA to reduce growth of *E. coli* and *S. aureus* in beef patties. *J. Food Sci.* **87**, 4569–4579 (2022).
78. Elsebaie, E. M. et al. Effects of Faba bean hull nanoparticles on physical properties, protein and lipid oxidation, colour degradation, and Microbiological stability of burgers under refrigerated storage. *Antioxidants* **11**, 938 (2022).
79. Zamora, R. & Hidalgo, F. J. Carbonyl–phenol adducts: an alternative sink for reactive and potentially toxic lipid oxidation products. *J. Agric. Food Chem.* **66**, 1320–1324 (2018).
80. Babolanimogadam, N. et al. Shelf life extending of probiotic beef patties with polylactic acid-ajwain essential oil films and stress effects on *Bacillus coagulans*. *J. Food Sci.* **89**, 866–880 (2024).
81. Barbieri, S. et al. Improved oxidative stability and sensory quality of beef hamburgers enriched with a phenolic extract from Olive vegetation water. *Antioxidants* **10**, 1969 (2021).
82. Majd, A. A. & Alrubeii, A. M. S. Al–Hadedee, L. T. The use of electrospun iron oxide nanofibers in coating frozen beefburger. *Iraqi J. Agric. Sci.* **55**, 1170–1177 (2024).
83. Amiri, E., Aminzare, M., Azar, H. H. & Mehrasbi, M. R. Combined antioxidant and sensory effects of corn starch films with nanoemulsion of *Zataria multiflora* essential oil fortified with cinnamaldehyde on fresh ground beef patties. *Meat Sci.* **153**, 66–74 (2019).
84. Zeb, A. & Ullah, F. A Simple spectrophotometric method for the determination of thiobarbituric acid reactive substances in fried fast foods. *J. Anal. Methods Chem.* 9412767 (2016).

85. Lin, L. et al. Preparation and characterization of gelatin active packaging film loaded with Eugenol nanoparticles and its application in chicken preservation. *Food Biosci.* **53**, 102778 (2023).
86. Lin, L., Mao, X., Sun, Y., Rajivgandhi, G. & Cui, H. Antibacterial properties of nanofibers containing chrysanthemum essential oil and their application as beef packaging. *Int. J. Food Microbiol.* **292**, 21–30 (2019).
87. Azarifar, M., Ghanbarzadeh, B., Sowti khiabani, M., Akhondzadeh basti, A. & Abdulkhani, A. The effects of gelatin-CMC films incorporated with Chitin nanofiber and *Trachyspermum Ammi* essential oil on the shelf life characteristics of refrigerated Raw beef. *Int. J. Food Microbiol.* **318**, 108493 (2020).
88. Barbosa-Pereira, L., Aurrekoetxea, G. P., Angulo, I., Paseiro-Losada, P. & Cruz, J. M. Development of new active packaging films coated with natural phenolic compounds to improve the oxidative stability of beef. *Meat Sci.* **97**, 249–254 (2014).
89. Erdem, A. K., Saglam, D., Ozer, D. & Ozcelık, E. Microbiological quality of minced meat samples marketed in Istanbul. *Van Vet. J.* **25**, 67–70 (2014).
90. Tunç, K. & Hoş, A. A study on ground meat microflora. *Ecol. Life Sci.* **9**, 15–18 (2014).
91. Doğan, C., Doğan, N., Gungor, M., Eticha, A. K. & Akgul, Y. Novel active food packaging based on centrifugally spun nanofibers containing lavender essential oil: rapid fabrication, characterization, and application to preserve of minced lamb meat. *Food Packag. Shelf Life* **34**, 100942 (2022).
92. Yilmaz, M. T., Hassanein, W. S., Alkabaa, A. S. & Ceylan, Z. Electrospun eugenol-loaded gelatin nanofibers as bioactive packaging materials to preserve quality characteristics of beef. *Food Packag. Shelf Life* **34**, 100968 (2022).
93. Patarata, L., Novais, M., Fraqueza, M. J. & Silva, J. A. Influence of meat spoilage microbiota initial load on the growth and survival of three pathogens on a naturally fermented sausage. *Foods* **9**, 676 (2020).
94. Alsammarraie, F. K., Lin, M. & Mustapha, A. Green synthesis of silver nanomaterials and evaluation of their antibacterial and antioxidant effectiveness in chicken meat. *Food Biosci.* **56**, 103332 (2023).
95. Committee, E. S. Guidance on the risk assessment of the application of nanoscience and nanotechnologies in the food and feed chain. *EFSA J.* **9**, 2140 (2011).
96. Ton-That, P. et al. Novel packaging Chitosan film decorated with green-synthesized nanosilver derived from Dragon fruit stem. *Food Hydrocoll.* **158**, 110496 (2025).
97. Cheng, J. et al. Preparation of a multifunctional silver nanoparticles polylactic acid food packaging film using mango peel extract. *Int. J. Biol. Macromol.* **188**, 678–688 (2021).

Acknowledgements

The authors would like to express their sincere gratitude to the Erciyes University Scientific Research Projects Unit for financial support under Project Number FDK-2023-13171.

Author contributions

Burcu Sarı Gençağ: Conceptualization, methodology, experimental work, data analysis, and writing of the main manuscript. Lütfiye Ekici and Kevser Kahraman: Supervision, project administration, and critical review of the manuscript. All authors have read and approved the final version of the manuscript.

Declarations

Competing interests

The authors declare no competing interests.

Additional information

Correspondence and requests for materials should be addressed to B.S.G.